Dynamics of the $^{16}O+^{16}O \rightarrow ^{32}S$ fusion process

P.-G. Reinhard* and J. Friedrich
Institut für Kernphysik, Johannes-Gutenberg-Universität, D-6500 Mainz, Federal Republic of Germany

K. Goeke and F. Grümmer
Institut für Kernphysik, Kernforschungsanlage Jülich, D-5170 Jülich, Federal Republic of Germany

D. H. E. Gross
Bereich Kern- und Strahlenphysik, Hahn-Meitner-Institut für Kernforschung, D-1000 Berlin, Federal Republic of Germany and Fachbereich Physik der Freien Universität Berlin, D-1000 Berlin, Federal Republic of Germany

(Received 16 March 1984)

The collective mass and potential, the quantum corrections, and the inertia parameters of the $^{16}O+^{16}O \rightarrow ^{32}S$ system are evaluated by means of the quantized adiabatic time dependent Hartree-Fock theory in a three-dimensional coordinate and momentum lattice. The interaction used, consisting of a direct finite range Yukawa force and a density-dependent term, is fitted by static Hartree-Fock calculations (including center-of-mass corrections) to binding energies and elastic electron scattering form factors in the mass region of interest here. The result of the fit is a new interaction, still without exchange terms, which for light nuclei reproduces the binding energies, the diffraction radii, and the surface widths. The sub-barrier fusion cross section for $^{16}O+^{16}O \rightarrow ^{32}S$ calculated with this force in quantized adiabatic time dependent Hartree-Fock theory is in excellent agreement with experimental data in contrast to calculations using other interactions. For the evaluation of the fusion cross section above the barrier classical trajectory calculations are performed using a suitable phenomenological friction force. This yields agreement with experimental data up to energies of 40 MeV above the barrier. The quantum corrections and the dependence of the mass parameter on the fragment distance are shown to have an important impact only below the barrier.

I. INTRODUCTION

In recent years the description of fusion between light and medium-heavy ions has attracted the interest of theoreticians, since here, in contrast to other heavy-ion processes, the reaction channel is well defined, and this is very important for the application of mean field methods. Furthermore, for not too heavy systems, these microscopic theories can be applied without larger technical limitations, thus allowing clean conclusions about the applicability of the theory. In the case of sub-barrier fusion, also tunneling properties of the many-body system are relevant which require the formulation of quantization prescriptions in self-bound systems. Furthermore, this process is particularly interesting, since adiabatic approximations made obviously or more or less implicitly in various many-body theories are certainly best fulfilled in the vicinity of or below the barrier. Therefore these assumptions should be checked here before they are applied to other fields like the description of thermonuclear burning rates at energies where experiments are at present not feasible.

Recently, sub-barrier fusion cross sections have been calculated for the $^{16}O+^{16}O \rightarrow ^{32}S$ system[1,2] by means of the quantized adiabatic time dependent Hartree-Fock theory (ATDHF) using the Bonche-Koonin-Negele interaction[3] (BKN). As a matter of fact, the experimental data have not been reproduced by the calculations, neither in magnitude nor in energy dependence. Since, besides adiabatic assumptions, the quantized ATDHF theory is based on variational methods and hence is free of adjustable parameters, the question arose if the failure is due to the adiabatic approximations, present also in many other theories, or to the interaction used. Furthermore, the question arose to which extent, by the inclusion of friction forces, fusion cross sections above the barrier can be reproduced by an adiabatic approach.

The present paper addresses both questions. We first show that one can indeed find an appropriate generalization of the BKN interaction which not only gives good binding energies and form parameters, but which also reproduces well the measured sub-barrier fusion cross sections within a quantized ATDHF calculation. Second, we show that, using a suitable phenomenological friction force and the adiabatically evaluated potential and mass parameter, fusion cross sections measured up to five times the barrier height are reproduced.

The paper is organized as follows. In Sec. II the quantized ATDHF method is briefly reviewed. Section III describes the generalization of the BKN interaction and the procedure we used to redetermine the free parameters by a fit to appropriate experimental data. In Sec. IV the collective potentials and the mass parameters calculated with BKN and with the new reaction are presented. Section V is devoted to the sub-barrier fusion cross section and the astrophysical S factor of the $^{16}O+^{16}O$ reaction. In Sec. VI, classical trajectory calculations involving the mass parameter and the potential energy surface calculated by quantized ATDHF are performed using a suitable friction

force. We discuss the effect of quantum corrections below and above the Coulomb barrier. The conclusions are summarized in Sec. VII.

II. QUANTIZED ATDHF

The details of the quantized ATDHF theory can be found in Refs. 4 and 5 and in the references given therein. Here we shall only briefly sketch the basic ideas and formulae.

The stationary wave function for the collective motion of the fragments towards each other is given by

$$\Psi(\vec{r}_1,\ldots,\vec{r}_A)=\int dq\,dp\,f(q,p)\Phi_{qp}(\vec{r}_1,\ldots,\vec{r}_A)\ . \tag{2.1}$$

Here the $|\Phi_{qp}\rangle$ are Slater determinants labeled conveniently by the distance $q=R$ of the two fragments with respect to each other and by the conjugate momentum $p=M(q)\dot{q}$. The p is included in the integrand to ensure a proper description of the dynamics in analogy to the double projection formalism of Goeke and Reinhard.[6] The adiabatic approximation involves the definition of a 1p-1h and 1h-1p operator $\hat{Q}(q)$ for the construction of the momentum p as

$$|\Phi_{qp}\rangle=[1+ip\hat{Q}(q)]\,|\Phi_q\rangle\ . \tag{2.2}$$

The variation of the total energy with respect to $\langle\Phi_{qp}|$, i.e.,

$$\delta_\Phi\langle\Psi|H-E|\Psi\rangle=0\ , \tag{2.3}$$

yields, after a lengthy algebra and with the Gaussian overlap approximation, the equation for the collective path (ATDHF equation):[7]

$$\frac{d}{dq}|\Phi_q\rangle=c(q)[\hat{H},\hat{H}_{ph}(q)]_{ph}(q)\,|\Phi_q\rangle\ , \tag{2.4}$$

with $c(q)$ given below. If one also performs a variation of $\langle\Psi|H-E|\Psi\rangle$ with respect to f^*, i.e.,

$$\delta_f\langle\Psi|\hat{H}-E|\Psi\rangle=0\ , \tag{2.5}$$

one obtains, again by Gaussian overlap techniques, a Schrödinger equation for the collective motion of the Lth partial wave:

$$H_c\left[q,\frac{d}{dq}\right]=-\frac{d}{dq}\frac{\hbar^2}{2M(q)}\frac{d}{dq}+V(q)-Z(q)+\frac{\hbar^2}{2\Theta(q)}L(L+1)\ . \tag{2.6}$$

In the above equations the index ph indicates the 1p-1h and 1h-1p part of an operator with respect to $|\Phi_q\rangle$. The $\hat{Q}(q)$ is given by

$$\hat{Q}(q)=\left[\frac{\partial V}{\partial q}\right]^{-1}\hat{H}_{ph}(q)\ , \tag{2.7}$$

with the classical potential

$$V(q)=\langle\Phi_q|\hat{H}|\Phi_q\rangle\ . \tag{2.8}$$

The mass parameter $M(q)$ reads as

$$\hbar^2/M(q)=\langle\Phi_q|[\hat{Q},[\hat{H},\hat{Q}]]|\Phi_q\rangle\ . \tag{2.9}$$

The quantum corrections $Z(q)$ include zero point energy corrections of the collective q motion and the spurious rotations and translations of the total system:

$$\begin{aligned}Z(q)=&[\hbar^2/2M(q)]\langle\Phi_q|(\overleftarrow{\partial}/\partial q)\vec{\partial}/\partial q\,|\Phi_q\rangle\\&+\tfrac{1}{2}\langle\Phi_q|\hat{Q}^2|\Phi_q\rangle\partial^2V/\partial q^2\\&+\sum_{i=1}^{3}\{[\hbar^2/2\Theta_i(q)]\langle\Phi_q|J_i^2|\Phi_q\rangle\\&\qquad+(\hbar^2/2mA)\langle\Phi_q|\nabla_i^2|\Phi_q\rangle\}\ .\end{aligned} \tag{2.10}$$

The $c(q)$ in Eq. (2.4) is given by $c(q)=M(q)/(\partial V/\partial q)$. It depends on the way the label q is chosen; the final results, however, are independent of this choice. Thus we can choose it at our convenience. For heavy ion fusion processes, involving A particles, we use a prescription which gives for separate ions the distance R between the fragments:

$$\tfrac{1}{2}AR^2=\langle\Phi_q|r^2Y_{20}|\Phi_q\rangle+\langle Q\rangle_1+\langle Q\rangle_2\ , \tag{2.11}$$

where $\langle Q\rangle_1$ and $\langle Q\rangle_2$ are the quadrupole moments of the isolated fragments. Actually, Eq. (2.4) poses an initial value problem and many different paths may be produced by using different initial conditions. Exploiting the validity condition[8] of quantized ATDHF it has been shown[3] that in case of fusion and fission processes the saddle point is the appropriate initial condition.

The actual solution of Eq. (2.4) is done by finite step methods yielding a discrete series of points q_n and states $|\Phi_n\rangle$. Here, it is most convenient to choose δq such that $c(q)\delta q=-\epsilon=$constant. This yields for the single particle wave functions $\varphi_\alpha^{(n)}(\vec{r})$, associated to $|\Phi_n\rangle$, the basic ATDHF equation in a three-dimensional $\vec{r}$ grid

$$\begin{aligned}\varphi_\alpha^{(n+1)}(\vec{r})=&\varphi_\alpha^{(n)}(\vec{r})-\epsilon[1-\rho_0(n)]\\&\times\{W_1(n)+W_0(n)[1-2\rho_0(n)]W_0(n)\}\\&\times\varphi_\alpha^{(n)}(\vec{r})\ .\end{aligned} \tag{2.12}$$

Here, $\rho_0(n)$ is the density matrix associated to $|\Phi_n\rangle$:

$$\langle\vec{r}\,|\rho_0(n)|\,\vec{r}\,'\rangle=\sum_{\alpha=1}^{A}\varphi_\alpha^{(n)}(\vec{r})\varphi_\alpha^{(n)}(\vec{r}\,')^*\ . \tag{2.13}$$

The $W_0(n)$ and $W_1(n)$ are given by

$$W_0(n)=-\frac{\hbar^2}{2m}\nabla^2+\mathrm{Tr}v\rho_0(n)\ , \tag{2.14}$$

$$W_1(n)=\mathrm{Tr}v[W_0(n),\rho_0(n)]\ . \tag{2.15}$$

The BKN force and its generalization, to be introduced below, do not show a momentum dependence, thus they have an effective mass $m^*/m=1$ and $W_1(n)=0$.

Actually, depending on which side of the saddle point one starts with $|\Phi_{n=0}\rangle$, the states $|\Phi_n\rangle$ approach for $n\rightarrow\infty$ the Hartree-Fock point of the compound nucleus or the asymptotic state of two fragments, which are near-

ly Hartree-Fock states interacting via the Coulomb force at slowly increasing distance. Hence, with $n\to\infty$ in each of two calculations, the full potential energy surface, mass parameters, etc., are evaluated. If one is only interested in obtaining the Hartree-Fock state one can use an approximation for Eq. (2.12)

$$\varphi_\alpha^{(n+1)}(\vec{r})=\varphi_\alpha^{(n)}(\vec{r})-\epsilon W_0(n)\varphi_\alpha^{(n)}(\vec{r})\ , \tag{2.16}$$

which is also known as the "gradient method" or "imaginary time-step method." The Hartree-Fock calculations in the next section are performed with this approximation, improved by accelerating techniques.[9]

III. THE TWO-BODY INTERACTION

At present, dynamical calculations in three-dimensional grids can only be performed using rather simple effective forces without exchange terms. An interaction which has been in use for several years was introduced by Bonche, Koonin, and Negele.[3] For a given one-body density distribution $\rho_0(\vec{r})$, normalized to the total nucleon number, the corresponding energy density reads

$$E(\vec{r})=\frac{\hbar^2}{2m}t_0(\vec{r})+\tfrac{3}{8}t_0\rho_0^2(\vec{r})+\tfrac{1}{16}t_3\rho_0^{\alpha+2}(\vec{r})+\tfrac{1}{2}V_y\rho_0(\vec{r})\int\frac{\exp(-|\vec{r}-\vec{r}'|/a)}{|\vec{r}-\vec{r}'|/a}\rho_0(\vec{r}')d^3\vec{r}'$$
$$+\tfrac{1}{8}e^2\rho_0(\vec{r})\int\frac{\rho_0(\vec{r}')}{|\vec{r}-\vec{r}'|}d^3\vec{r}'\ . \tag{3.1}$$

Here, we have introduced the free parameter α in the density dependent term; the original BKN force had $\alpha=1$.

The corresponding Hartree-Fock Hamiltonian is given by

$$W_0(\vec{r},\vec{r}')=\delta(\vec{r}-\vec{r}')\left[-\frac{\hbar^2}{2m}\nabla^2+\tfrac{3}{4}t_0\rho_0(\vec{r})+\tfrac{1}{16}(\alpha+2)t_3\rho_0^{\alpha+1}(\vec{r})\right]$$
$$+V_y\int\rho_0(\vec{r})\frac{\exp(-|\vec{r}-\vec{r}'|/a)}{|\vec{r}-\vec{r}'|/a}\rho_0(\vec{r}')d^3\vec{r}\,d^3\vec{r}'+\tfrac{1}{4}e^2\int\frac{\rho_0(\vec{r}')}{|\vec{r}-\vec{r}'|}d^3\vec{r}'\ . \tag{3.2}$$

The total energy is given either by

$$E=\langle\Phi_{\rm HF}|\hat{H}|\Phi_{\rm HF}\rangle=\int E(\vec{r})d^3r \tag{3.3}$$

or by

$$E=\tfrac{1}{2}\sum_{\alpha=1}^{A}\langle\varphi_\alpha|-\frac{\hbar^2}{2m}\nabla^2+W_0|\varphi_\alpha\rangle+E_R\ , \tag{3.4}$$

with the rearrangement energy

$$E_R=-\alpha\frac{t_3}{32}\int d^3r\,\rho^{\alpha+2}(\vec{r})\ . \tag{3.5}$$

Actually, in most applications in the literature the BKN interaction is used without applying center-of-mass corrections to the Hartree-Fock ground state and ignoring the Coulomb force, although both effects are not negligible for single nuclei as well as for heavy ion systems. One may take them into account by considering as ground state energy

$$E_{\rm g.s.}=\langle\Phi_{\rm HF}|\hat{H}|\Phi_{\rm HF}\rangle-\frac{\hbar^2}{2mA}\langle\Phi_{\rm HF}|\vec{\nabla}^2|\Phi_{\rm HF}\rangle$$
$$-\sum_{i=1}^{3}\frac{\hbar^2}{2\Theta_i}\langle\Phi_{\rm HF}|\vec{J}_i^{\,2}|\Phi_{\rm HF}\rangle\ , \tag{3.6}$$

where the direct Coulomb part is contained in $\hat{H}$. With the last term in Eq. (3.6) we also take into consideration rotational corrections which must be applied to deformed nuclei.

The fusion process is governed by the energy of the fragments and compound nucleus and by the spatial mass distribution functions of the nuclei. The appropriateness of the interaction for the description of this process should therefore be given by the reliability with which the interaction reproduces the relevant measured quantities. We have checked the quality of the parametrization given by Bonche, Koonin, and Negele[3] as well as that given by Köhler[10] by comparing the calculated values to experiment in the mass region of interest here, i.e., for $A\leq 40$. For the sake of completeness we have compiled their parameter values in columns 3 and 4 of Table I.

In addition to the binding energy E, we look for the form of the density distribution. The fusion process under investigation is certainly dominated by the extension and by the surface width of the distributions. In particular, the latter quantity should play an important role since it is the strong interaction of overlapping tails which helps to overcome the Coulomb repulsion. As a measure for the nuclear extension we take the diffraction radius R_d. This radius is determined from the momentum transfer k_1 of the first diffraction minimum in the elastic

TABLE I. Parameter values of the finite-range Yukawa interaction (Ref. 3). The resulting Hartree-Fock Hamiltonian and the total energy are given in Eqs. (3.1) and (3.2), respectively.

	This paper	BKN (Ref. 3)	Köhler (Ref. 8)
α	0.25	1.00	0.33
t_0 (MeV fm^3)	0.	−497.73	−1072.14
t_3 (MeV fm$^{3+\alpha}$)	14316.2	17270.0	14203.0
V_y (MeV)	−5998.64	−363.044	−517.01
a (fm)	0.2786	0.4598	0.4598

electron scattering form factor in the spirit of Helm's model[12] for the charge distribution, i.e., $R_d = 4.493/k_1$, as described in Ref. 11. This radius corresponds to the droplet-model radius; for light nuclei it has a value of approximately $1.12A^{1/3}$ fm. The surface width σ is extracted from the height and the position of the second form factor maximum according to the prescription given in Eq. (12) in Ref. 11. In that definition it has a value around 0.9 fm, being systematically smaller for light nuclei. In Fig. 1 we also compare the calculations to the more familiar rms radius. In the picture of the Helm model[12] the form parameters are related to each other by

$$\langle r^2 \rangle = \tfrac{3}{5} R_d^2 [1 + 5(\sigma/R_d)^2] \, . \tag{3.7}$$

Equation (3.7) shows that the rms radius mixes up the information about the nuclear extension R_d with that about the surface width σ, in particular, in light nuclei where σ is comparable to R_d. In Fig. 1 we show results for $4n$ nuclei between ^{4}He and ^{40}Ca.

One realizes underbinding of 5% to 12% for $16 \leq A \leq 40$ and about 23% for ^{12}C. Since these deficiencies are strongly A dependent one is bound to obtain poor potential energy surfaces for heavy-ion collisions since fragments and compound states are not equally well (or poorly) described. Apparently, Köhler's force is not of better quality in this respect.

The nuclei are predicted by both the BKN and the Köhler force to have too large extension R_d. The BKN force gives substantially too small surface widths. With this force the two deficiencies in the extension parameters R_d and σ just cancel in the determination of the rms radius which, for ^{16}O and ^{40}Ca, is reproduced extremely well by this force. However, the small surface width is bound to yield too large Coulomb barrier heights in heavy-ion collisions and therefore strongly suppresses sub-barrier fusion. The Köhler parametrization gives a good surface width; the poor reproduction of the rms radii is only due to that in R_d.

TABLE II. Height and position of the barrier. The position R_B and height H_B of the barrier are given for the new set of parameters given in Table I, for the parameters from Ref. 3, and for a phenomenological potential fitted to fusion data involving *sd*-shell fragments.

	This paper	BKN (Ref. 3)	Phenomenological (Ref. 23)
R_B (fm)	8.53	8.16	8.6
H_B (MeV)	10.07	10.59	10.0

In order to improve upon the BKN parametrization we increased the flexibility by introducing the free parameter α in the density dependent term and then determined the five free parameters α, t_0, t_3, V_y, and a by fitting them to the relevant measureable observables E, R_d, and σ in ^{16}O and ^{40}Ca in a χ^2 minimizing procedure.[13] The experimental values are taken from Refs. 14 and 11. The calculation for the fit is performed with a fast Hartree-Fock code where we also take into account the direct part of the Coulomb interaction and where we correct the total energy by subtracting the translational spurious energy. The resulting density distribution is then Fourier transformed to give the form factor from which we extract the form parameters R_d and σ just as it is done with the experimentally determined charge distributions.[11] The finite ex-

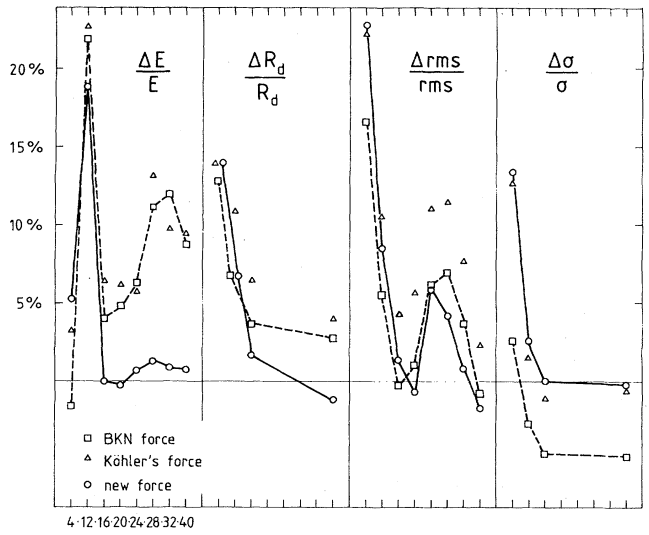

FIG. 1. Binding energy, diffraction radius, rms radius, and surface width: relative deviation between experimental values and calculations with different finite-range Yukawa interactions. The Hartree-Fock calculations include the direct Coulomb force and center-of-mass corrections. Positive values of $\Delta E/E$ indicate underbinding. The diffraction radius and the surface width are determined by means of the elastic electron scattering form factor (see the text for details).

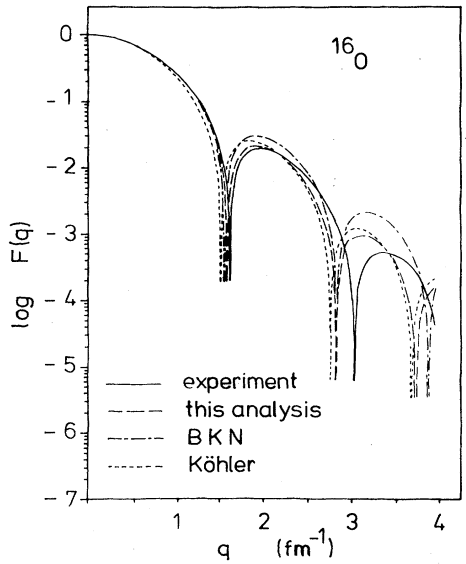

FIG. 2. The elastic electron scattering form factor of ^{16}O defined as the Fourier transform of the charge distribution. The experimental result is taken from Ref. 25. Köhler's force yields the largest diffraction radius (first minimum at the smallest momentum transfer), and the BKN parameters yield the smallest surface width (largest form factor in the second maximum). The high Fourier components are not well reproduced by any of the forces.

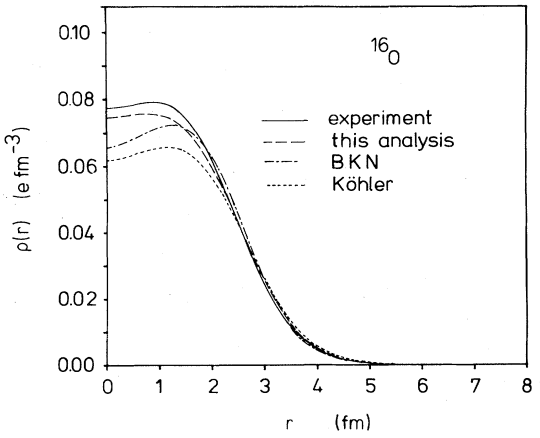

FIG. 3. The charge density of ^{16}O. Nomenclature as in Fig. 2.

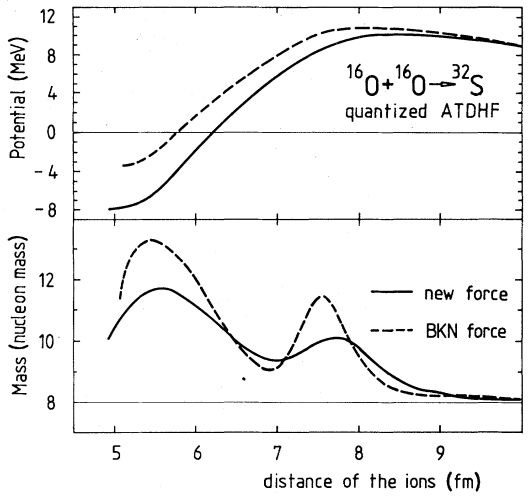

FIG. 4. The quantized ATDHF potential $V(R)-Z(R)$ and the mass parameter $M(R)$ for the $^{16}O + ^{16}O$ collision versus the distance R between the ions. The new parameter set yields a lower barrier height and (in agreement with the measured binding energy of ^{32}S) a stronger binding of the compound system. In addition, the mass parameter is less structured with the new force.

tension of the nucleons is taken into account appropriately.

Since both t_0 and V_y describe to some extent the same nuclear properties, the χ^2 minimum turns out to be extremely flat in the t_0-V_y plane having an asymptotic minimum for $t_0 \to +\infty$ and $V_y \to -\infty$. Since this asymptotic minimum is only slightly lower than the χ^2 value at small t_0 we have chosen arbitrarily the value $t_0 = 0$. The remaining four parameters are then determined by the minimum in χ^2. The resulting set of parameters is given in column 2 of Table II.

The new parametrization of the generalized BKN force, allowing for $\alpha \neq 1$, has a substantial effect on the nuclear ground state data of light nuclei as is demonstrated also in Fig. 1. For ^{16}O and ^{40}Ca all given data are noticeably better reproduced by the new interaction than by the others. For all $4n$ nuclei in the range $16 \leq A \leq 40$ the calculated binding energy deviates from the measured values by less than 2%. We do not show R_d and σ for the nuclei known to be deformed since here the spherical calculation is inappropriate, in particular, with respect to the surface width σ. For ^{16}O and ^{40}Ca one notices a lowering of the diffraction radius and an increase of the surface width with the new parametrization. The rms radius is comparable in quality to those calculated with the other two forces. The important distinction between the forces lies in their ability to reproduce extension and surface width separately. Actually, for ^{4}He and ^{12}C all interactions are rather poor (results for ^{8}Be are not given at all since this nucleus is unbound in nature whereas the ordinary microscopic forces yield a bound system).

In Figs. 2 and 3 we compare the charge distribution and its Fourier transform directly to the measured results. The improvement with the new set of parameters is clearly visible.

IV. COLLECTIVE MASS AND POTENTIAL

As an application of the new force to heavy ion collisions we consider the fusion process $^{16}O + ^{16}O \to ^{32}S$. Starting from the saddle point, the ATDHF equation [(2.4) or (2.12)] is solved by finite-step methods using a step size of $\Delta x = \Delta y = \Delta z = 1$ fm. Details of the Fourier components in the wave function for $\hbar^2 k^2/2m > 100$ MeV are ignored. Accordingly, ϵ is close to 10^{-4} MeV^{-2}. Further details of the numerical procedure can be found in Refs. 2 and 5.

In Fig. 4 we show the resulting mass parameter $M(R)$ and the quantum mechanical collective potential $V(R)-Z(R)$ for Eq. (2.6) calculated for both the BKN and the new parameter set. The collective mass parameters look somewhat similar for both forces. They have bumps at rather the same positions; their heights, however, are different. Apparently, in accordance with the larger surface width the changes of the internal wave functions take place over a larger range of distances between the two colliding nuclei and this leads to broader peaks with reduced heights. For the collective potential two features should be pointed out. First, the height of the barrier is reduced for the new force due to the noticeably larger surface width. Second, the potential with the new parameters is deeper for $R = 0$ due to the stronger binding of the ^{32}S nucleus (cf. Fig. 1) which is in agreement with the measured value. We shall see that the sum of all these effects changes the fusion cross section quite drastically.

We could also have performed calculations of the potential and the mass parameters using Köhler's force.[10] However, the calculations with the three-dimensional ATDHF code are rather time consuming and we preferred the BKN force for a detailed comparison since this force is mostly used in the literature. The larger surface width with Köhler's force should lead in the right direction.

V. SUB-BARRIER FUSION CROSS SECTION

Having evaluated $V(R)$, $Z(R)$, $M(R)$, and $\Theta(R)$ for the $^{16}O + ^{16}O\rightarrow^{32}S$ system the full Hamiltonian is available. From this the sub-barrier fusion cross section can be calculated by generalized WKB techniques. The transmission coefficient at the c.m. energy $E_{c.m.}$ is given by

$$T_L(E_{c.m.})=[1+\exp(2I_L)]^{-1}\,, \tag{5.1}$$

with

$$I_L(E_{c.m.})=\int_a^b([2M(R)/\hbar^2]\{V(R)-Z(R)+[\hbar^2/2\Theta(R)]L(L+1)-E_{c.m.}\})^{1/2}dR\,, \tag{5.2}$$

where a and b are the classical turning points.

The fusion cross section for identical incident nuclei is then given by

$$\sigma_{fus}(E_{c.m.})=\frac{\pi\hbar^2}{2\mu E_{c.m.}}\sum_L[1+(-)^L](2L+1)T_L(E_{c.m.})\,. \tag{5.3}$$

Instead of σ_{fus}, below the barrier one normally refers to the astrophysical S factor defined by

$$S(E_{c.m.})=E_{c.m.}\sigma_{fus}(E_{c.m.})\exp(2\pi Z_1Z_2e^2/\hbar v)\,, \tag{5.4}$$

where v is the relative velocity of the ions. The astrophysical S factor is preferred for sub-barrier fusion since one thus takes out the dropping by several tens of orders of magnitude present in the cross section due to the trivial penetration through the Coulomb barrier; thus the S factor reveals in a more transparent way the influence of the nucleon-nucleon interaction.

In Fig. 5 we show the astrophysical S factor for the reaction under discussion, again calculated with both the BKN and the new parameter set: one realizes a drastic effect on the S factor. With the new parameters, the S factor is larger by a factor ranging from 2 at $E_{c.m.}=10$ MeV up to 4 at the lowest measured energy of $E_{c.m.}=7$ MeV. The agreement with the measured data is not so good that we must emphasize here that the parameters have not been fitted to these data, nor to any data of this kind. In contrast, they have just been fitted to appropriate information on ground state charge distributions available

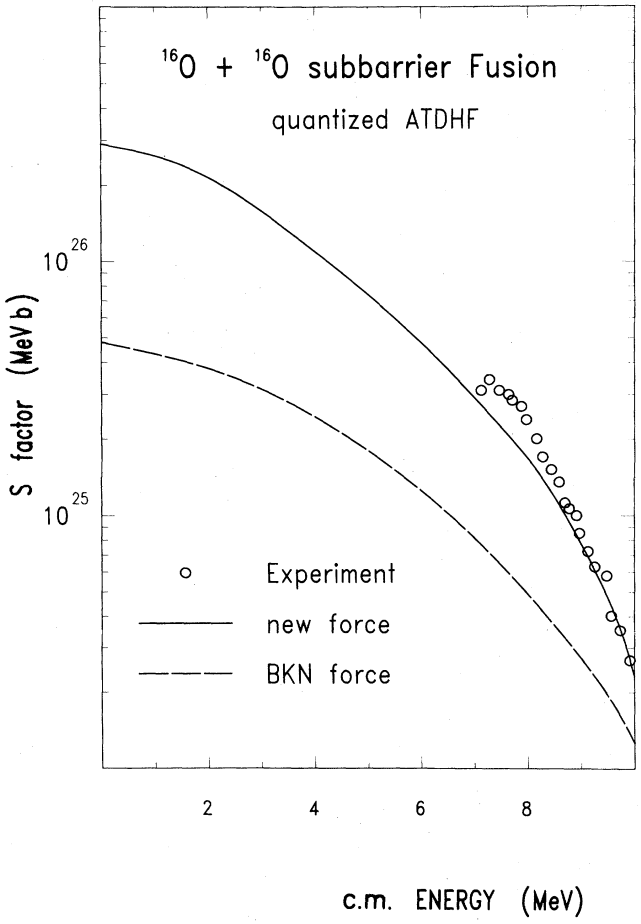

FIG. 5. The astrophysical S factor for the sub-barrier fusion of $^{16}O + ^{16}O$. The nomenclature for the curves as in Fig. 4. The data points are taken from Ref. 24. Note that the continuous curve is not fitted to these data.

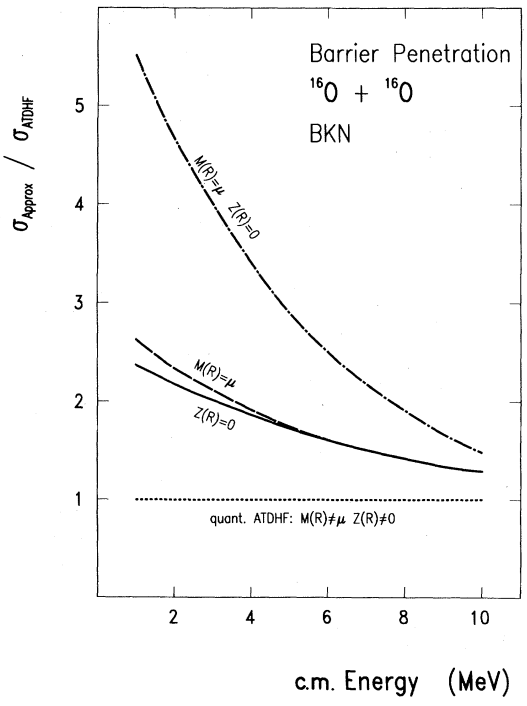

FIG. 6. The sub-barrier fusion cross section calculated with various approximations compared to the full quantized ATDHF result. The approximations indicated on the different curves refer to the corresponding approximations in the evaluation of the transmission coefficient with Eqs. (5.1) and (5.2).

from elastic electron scattering cross sections.

It is interesting to investigate the effect of the variation of M with R, i.e., the deviation of the mass parameter M from the reduced mass of the system, and the importance of the quantum corrections $Z(R)$ for the sub-barrier fusion cross section. In Fig. 6 we show various approximately evaluated cross sections as their ratio to the quantized ATDHF calculation versus center-of-mass energy. The approximations concern the various terms in the penetration integral of Eq. (4.2). It is obvious that at energies well below the barrier it is indispensable to account for the R-dependent mass $M(R)$ and for the quantum corrections $Z(R)$. These findings, which have already been discussed by Urbano *et al.*[15] in a simple model, are particularly important for the evaluation of thermonuclear burning rates.

VI. FUSION ABOVE THE BARRIER

The fusion above the barrier cannot be calculated reliably by penetration models since besides fusion and elastic scattering many excitation channels are open giving rise to dissipative effects. A reasonable approximation consists of a classical trajectory calculation using a phenomenological friction force. If for a certain relative angular momentum L the trajectory is trapped for an energy $E_{\text{c.m.}}$, one assumes for the transmission coefficient $T_L(E_{\text{c.m.}})=1$, otherwise $T_L=0$. The final fusion cross section is then again calculated by Eq. (4.3).

For the present calculation we apply the model of Gross and Kalinowski[16] which uses the equation of motion

$$\frac{d}{dt}[M(R)\dot{R}]-\frac{1}{2}\frac{dM}{dR}\dot{R}^2-\frac{1}{2}\frac{d\Theta}{dR}\dot{\varphi}^2+\frac{d(V-Z)}{dR}+K_R\dot{R}=0\,, \tag{6.1}$$

$$\frac{d}{dt}[\Theta(R)\dot{\varphi}]+K_\varphi\dot{\varphi}=0\,. \tag{6.2}$$

Here, K_R and K_φ are the radial and tangential friction coefficients, respectively. The main energy loss is described by Eq. (6.1). Equation (6.2) describes the loss of angular momentum connected with some additional loss of (rotational) energy; angular momentum is conserved in the fusion channel if $K_\varphi=0$. The friction coefficients are parametrized as

$$K_R=K_R^0(\nabla V_{\text{fr}})^2,\quad K_\varphi=K_\varphi^0(\nabla V_{\text{fr}})^2\,. \tag{6.3}$$

Here, V_{fr} measures the geometrical overlap of the single particle potential of the target with the nucleon density of the projectile[16]

$$V_{\text{fr}}(\vec{\mathrm{R}})=\int V_1(\vec{\mathrm{R}}-\vec{\mathrm{r}})\rho_2(\vec{\mathrm{r}})d^3r\,, \tag{6.4}$$

with V_1 and ρ_2 having Saxon-Woods shape:

$$V_1(\vec{\mathrm{r}})=\alpha_1/\{1+\exp[(\vec{\mathrm{r}}-\beta_1)/\gamma_1]\}\,, \tag{6.5a}$$

$$\rho_2(\vec{\mathrm{r}})=\alpha_2/\{1+\exp[(\vec{\mathrm{r}}-\beta_2)/\gamma_2]\}\,. \tag{6.5b}$$

The parameters are $\alpha_1=-50$ MeV, $\beta_1=1.25A_1^{1/3}$ fm, $\gamma_1=0.65$ fm, and $\alpha_2=0.17$ fm, $\beta_2=1.12A_2^{1/3}-0.86A_2^{-1/3}$, $\gamma_2=0.54$ fm.

The trajectory calculations are performed with the friction coefficients $K_R^0=4\times10^{-23}$ sec MeV^{-1} and $K_\varphi^0=0.01\times10^{-23}$ sec MeV^{-1}. The resulting fusion cross sections are shown in Fig. 7. Again, the $V(R)$ and $Z(R)$ have been calculated with the BKN parameters and also with the new interaction determined in this paper. The theoretical curves in Fig. 7 are to be compared with the experimental data[17–22] whose spreading is due to different evaporation residues considered. As in the case of sub-barrier fusion the new parameters give good agreement with the experimental data, whereas the BKN force again yields too small cross sections. The differences again are due to the different surface properties and binding energies, which in particular lead to a higher saddle point for the BKN force which, obviously, is at variance with experiment. When stating this we take it as a second remarkable result that the adiabatic theory is applicable also above the barrier if a suitable friction force is used. In the present example the agreement with experimental data holds even for energies up to $E_{\text{c.m.}}=50$ MeV. Altogether it is clearly demonstrated that the microscopic and funda-

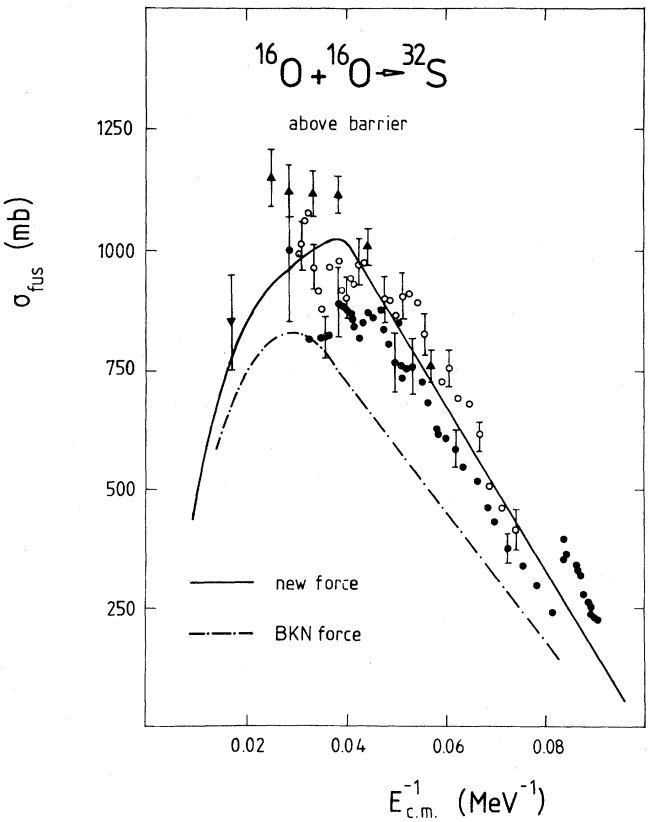

FIG. 7. Comparison of the theory with experiment for $^{16}O+^{16}O$ fusion above barrier as a function of the inverse of the center-of-mass energy. Both curves are obtained by trajectory calculations involving the quantized ATDHF potentials $V(R)-Z(R)$ and a phenomenological friction force (Ref. 16) fitted to the available fusion data of *sd*-shell nuclei. The calculation with the new parameter set is in excellent agreement with the data (for the scattering of the data see the text).

mental theory combined with a well founded phenomenological friction approach does work.

If one replaces in Eq. (6.1) the quantized ATDHF potential $V(R)-Z(R)$ by a phenomenological one-folding potential $U(R)$ of the form [Eqs. (6.4) and (6.5)] one obtains the phenomenological friction model of Gross and Kalinowski. A detailed comparison of this model with the experimental data on fusion above the barrier and on deep inelastic collisions has shown that the phenomenological nucleus-nucleus potential is well described by the one-folding formulae with parameters for the collision of *sd*-shell nuclei[16,23] $\alpha_1=-40$ MeV, $\beta_1=1.25A_1^{1/3}$ fm, and $\gamma_1=0.45$ fm, whereas the α_2, β_2, and γ_2 are as above. The agreement of the theoretical results with the fusion data measured above the barrier is good for available systems and qualitatively like the one shown in Fig. 7. This fitted phenomenological potential $U(R)$ is compared in Fig. 8 with that from the quantized ATDHF calculation, $V(R)-Z(R)$, and we find a striking agreement. This demonstrates that the single folding potential $U(R)$ includes realistically many-body effects as far as they are relevant for fusion above the barrier. Of course, particular systems can deviate from the average trends; then it is necessary to incorporate these deviations as discussed in Ref. 16. It is also interesting to note from Fig. 8 that the proximity potential calculated in Ref. 23 is only one-third of the quantized ATDHF and single folding potentials.

In Fig. 9 we demonstrate the effect of various approximations in Eqs. (6.1) and (6.2) by comparing the full solution to the approximations $M(R)=\mu$ (reduced mass) and $Z(R)=0$, respectively. One realizes that the three cases give rather similar results, in particular, as compared to

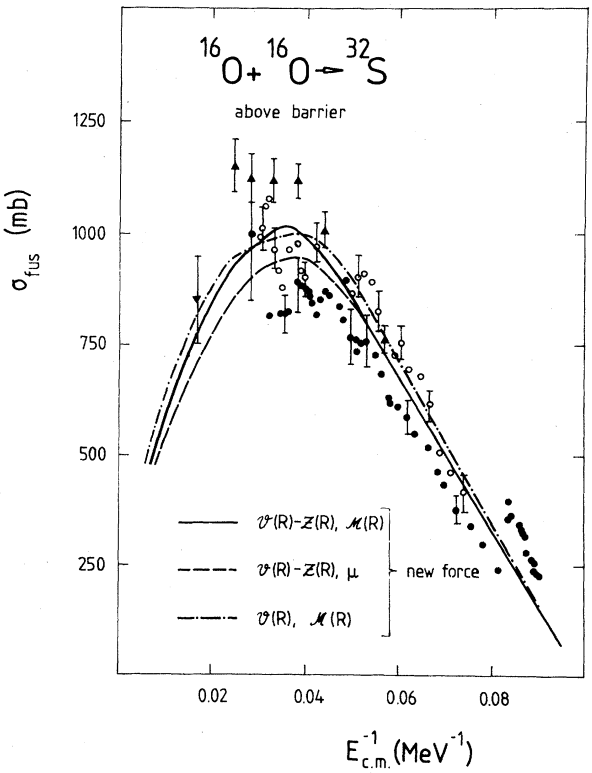

FIG. 9. Comparison of trajectory calculations involving various approximations with the full solution (full curve). The uncertainty in the data is larger than the difference between the different approximations, therefore any of the approximations is acceptable here.

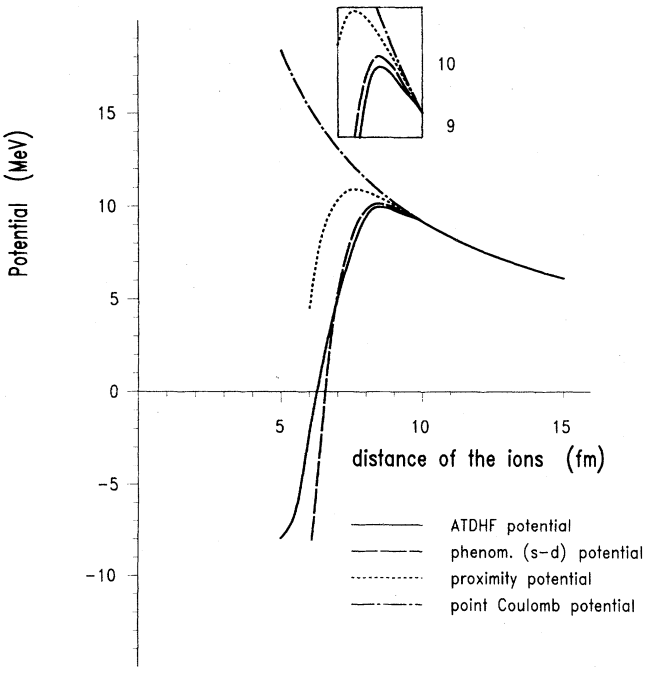

FIG. 8. Comparison between the quantized ATDHF potential for the $^{16}O+^{16}O$ collision, the proximity potential, and a phenomenological potential fitted to *sd*-shell nuclei (Ref. 23).

the scatter of the data. This shows that fusion cross sections above the barrier are not very sensitive to the mass parameter and also not to the slight deviations of $V-Z$ from V in the vicinity of the saddle point. Actually, this feature is quite different from the situation below the barrier, as has been discussed in the context on Fig. 6. The slight increase of the fusion cross section above the barrier with R-dependent mass $M(R)$ as compared to $M(R)=\mu$ can be understood easily. On the way in, the $M(R)$ is increasing with decreasing R, hence the force $-\frac{1}{2}(dM/dR)\dot{R}^2$ in Eq. (6.1) is positive and helps to overcome the friction and the Coulomb repulsion. Thus, the penetrability is enhanced yielding a larger fusion cross section.

VII. SUMMARY AND CONCLUSION

The present paper is concerned with the fusion cross section at low energies. The theoretical description of the process is based on three ingredients: (i) a suitable microscopic theory, (ii) a proper microscopic interaction, and (iii) an appropriate friction force for energies above the barrier. It turns out that, indeed, the experimental data can be reproduced surprisingly well from the lowest measured energies up to $E_{\text{c.m.}}=50$ MeV if each of the three ingredients is chosen carefully.

The microscopic theory is the quantized ATDHF ap-

proach which is solely based upon an adiabatic assumption and variational principles. Up to now it was by no means clear whether this was an appropriate approach to the problem since the calculations had failed to reproduce the measured data. Agreement with the sub-barrier data is achieved with this theoretical approach by using a suitably chosen interaction, namely a force which reproduces, in particular, the surface widths and the binding energies in the mass region of interest in the process, i.e., in particular for the compound nucleus and the incident fragments. This force is obtained by fitting the parameters of a generalized BKN interaction to measured binding energies and to elastic electron scattering form factors. In the latter we put emphasis on the nuclear extension and on surface properties as given by the diffraction radius and the surface width. In particular, the force is not fitted to the rms radius which only gives a mixture of extension and surface width. As a result of the fitting procedure, the power of the density in the density dependent term has been chosen as $\alpha=0.25$. It is this parameter which allows for larger surface widths in agreement with experiment. The new interaction yields a potential energy surface with a lower barrier at greater internucleus distance than that obtained with the Bonche-Koonin-Negele parametrization. This energy surface is in good agreement with phenomenological potentials fitted to fusion data of *sd*-shell fragments by means of trajectory calculations.

With this approach the sub-barrier data for $E_{\text{c.m.}}$ between 8.5 and 10 MeV are reproduced so precisely as if the calculation were fitted to these data. This not being the case, one might be allowed to take seriously the deviation between the calculation and the data around 7.5 MeV which now looks like a structure in the fusion cross section. Here one would like to have a few more data points at lower energies.

We have completed the approach to fusion by taking into account a phenomenologically determined friction force. Using this force in a trajectory calculation with the potential taken from the quantized ATDHF approach we also find agreement with experiment for fusion several tens of MeV above the barrier. Here, the quantum corrections and the dependence of the mass parameter on the internucleon distance do not play as an important role as they do in sub-barrier fusion.

---

*Present address: Institut für Theoretische Physik, Universität Erlangen, D-8520 Erlangen, Federal Republic of Germany.

[1]F. Grümmer, K. Goeke, and P.-G. Reinhard, in *Proceedings of the International Conference on Time Dependent Hartree-Fock and Beyond, Ban Honnef, 1982,* Lecture Notes in Physics, edited by K. Goeke and P.-G. Reinhard (Springer, Berlin, 1982), p. 323.

[2]K. Goeke, F. Grümmer, and P.-G. Reinhard, Phys. Lett. **124B**, 21 (1983).

[3]P. Bonche, S. Koonin, and J. Negele, Phys. Rev. C **13**, 1226 (1976).

[4]K. Goeke and P.-G. Reinhard, Ann. Phys. (N.Y.) **112**, 328 (1978).

[5]K. Goeke, F. Grümmer, and P.-G. Reinhard, Ann. Phys. (N.Y.) **150**, 504 (1983).

[6]K. Goeke and P.-G. Reinhard,, Ann. Phys. (N.Y.) **124**, 249 (1980).

[7]P.-G. Reinhard and K. Goeke, Phys. Rev. C **20**, 1546 (1979).

[8]P.-G. Reinhard and K. Goeke, Nucl. Phys. **A312**, 121 (1978).

[9]P.-G. Reinhard and R. Y. Cusson, Nucl. Phys. **A378**, 418 (1982).

[10]S. Köhler, Nucl. Phys. **A343**, 315 (1980).

[11]J. Friedrich and N. Voegler, Nucl. Phys. **A373**, 192 (1982).

[12]R. Helm, Phys. Rev. **104**, 1466 (1956); H. Uberall, *Electron Scattering from Complex Nuclei* (Academic, New York, 1971).

[13]J. Friedrich, P.-G. Reinhard, and N. Voegler (unpublished).

[14]J. H. E. Mattauch, W. Thiele, and A. H. Wapstra, Nucl. Phys. **67**, 1 (1965).

[15]J. N. Urbano, K. Goeke, and P.-G. Reinhard, Nucl. Phys. **A370**, 329 (1981).

[16]D. H. E. Gross and H. Kalinowski, Phys. Rev. C **45**, 175 (1978).

[17]A. Weidinger, F. Busch, G. Gaul, W. Trautmann, and W. Zipper, Nucl. Phys. **A263**, 511 (1976).

[18]B. Fernandez, C. Gaarde, J. S. Larsen, S. Pontoppidan, and F. Vidabaek, Nucl. Phys. **A306**, 259 (1978).

[19]H. Spinke and H. Winkler, Nucl. Phys. **A233**, 456 (1974).

[20]J. J. Kolata, R. C. Fuller, R. M. Freeman, F. Haas, B. Heusch, and A. Gallman, Phys. Rev. C **16**, 891 (1977).

[21]M. Conjeaud, S. Harar, F. Saint-Laurent, J. M. Loiseaux, J. Menet, and J. B. Viano, in Proceedings of the Symposium on Macroscopic Feaures of Heavy Ion Collisions and Pre-equilibrium Processes, Hakone, Japan, 1977, as quoted in J. R. Birkelund, L. E. Tubbs, J. R. Huizenga, J. N. De, and D. Sperber, Phys. Rep. C **56**, 107 (1979).

[22]I. Tserruya, Y. Eisen, D. Pelte, A. Gavron, H. Oeschler, D. Berndt, and H. L. Harney, Phys. Rev. C **18**, 1688 (1978).

[23]D. H. E. Gross and L. Satpathy, in *Nuclear Physics,* edited by C. H. Dasso, P. A. Broglia, and A. Winther (North-Holland, Amsterdam, 1982), p. 691; P. Fröbrich (unpublished).

[24]C. Rolfs and D. Trautvetter, Annu. Rev. Nucl. Part. Sci. **28**, 115 (1978).

[25]G. Lahm, Ph.D. dissertation, Universität Mainz, 1983; G. Lahm and R. Neuhausen (unpublished).